

Modelling and Co-Simulation of Small Wind Turbine with Permanent Magnet Synchronous Generator

Abstract. This paper presents the Co-Simulation of a Small Wind Turbine (SWT) with Permanent Magnet Synchronous Generator (PMSG). It combines Simulink, Maxwell and Simplorer software's to show the electrical machine behaviour connected with the power electronics' circuit. To the control of the system the Maximum Power Point Tracking (MPPT) algorithm is used. The finite element analysis (FEA) was used to design the novel electrical machine with permanent magnets. Application of FEA method for PMSG modelling guarantee exhibit a more accurate behaviour over simplified Simulink models, also during motor and power electronics faults.

Streszczenie. W artykule przedstawiono zagadnienie symulacji małej turbiny wiatrowej z generatorem synchronicznym z magnesami trwałymi (PMSG) przy wykorzystaniu trzech niezależnych środowisk programistycznych (tzw. współsymulacja). Podczas analizy wykorzystano wspólne obliczenia z programów Simulink, Maxwell i Simplorer. Model generatora wykonany został w środowisku Maxwell (z wykorzystaniem metody elementów skończonych (FEM)), co pozwala na jego dokładną analizę zarówno w stanach statycznych jak i dynamicznych. Układ energoelektroniki zamodelowano w programie Simplorer a układy sterowania (przy wykorzystaniu metody MPPT) w środowisku Simulink. Taka analiza pozwala na uzyskanie dokładnych rezytatów w różnych warunkach pracy – w tym podczas uszkodzenia maszyny lub elementów energoelektroniki. (Modelowanie i współsymulacja małej turbiny wiatrowej z generatorem PMSG).

Keywords: Modelling; Co-simulation; FEA; PMSG; MPPT; WECS.

Słowa kluczowe: Modelowanie; Co-symulacja; FEA; PMSG; MPPT; WECS.

Introduction

Electrical machines and electrical drives are modelled using different software. Most of them assumed that models of electrical machines are linear [1] or only the magnetizing characteristic is taken into account [2]. These methods are good for simple well – known electrical drives [3]. For new concept of electrical machines, the methods based on the FEA (Finite Element Analysis) should be adopted. The main disadvantage of that approach is long computational time.

In recent years the computational power increase along with the advancements in the coupling methods between different software calculations, namely co-simulation [4], has led to the development of better models of complex systems which include multiphysics' dynamics. One such a system is the wind turbine (WT), which has gained notoriety at different scales for specific applications.

One of the issues that requires exact calculations is the research related to small wind turbines (SWT). A SWT is normally used as a standalone system or in water pumping applications [5]. These small wind turbines (power less than 200 kW) are dominated by the use of permanent magnet synchronous generators (PMSG) [6], this is mainly because the lack of external excitation or additional energy input at starting and low speeds.

The co-simulation approach has been used in the design and analysis of complex machines like doubly salient permanent magnet (DSPM) motor for fault tolerance analysis (short circuit and open circuit phase) [7], also for the five-phase dual-rotor PMSM [8], in the design of standalone micro hydro 4 kW PMSG [9], for the fault analysis of permanent magnet motor, such as inter-turn short circuit faults [10], [11], in the induction motor (IM) for the analysis of broken rotor bar [12], in the analysis of core losses of the brushless DC motor (BLDCM) [13] and also in the design and fault analysis of a 120 kW PMSG for wind turbines [14] and in the interturn short circuit analysis of a 2 MW 60 pole PMSG for direct-drive wind turbine [15].

The literature shows very good agreement with previous work done mostly experimentally. Also, most of the aforementioned literature explain the advantages of using the co-simulation method for fault research, since the expenses of intentionally damaging such prototypes very quickly add up while trying different faults and sensitivities.

Even in the design phase of the wind energy conversion system (WECS) the advantages of using the co-simulation approach are present [9].

In this work the co-simulation of a small WECS is demonstrated and compared with results from the classical simulation with Matlab Simulink (Sim Power System).

In section 2 the classical model for the PMSG is displayed including the partially more complex trapezoidal model. In section 3, the wind turbine model based on Cp-lambda curve used for both simulation and co-simulation is presented. In section 4 the maximum power point tracking (MPPT) algorithm used in this work is shown. In section 5 the co-simulation methodology is presented. In section 6 the results of both simulation and co-simulation are demonstrated and compared and finally some conclusions from these comparisons are stated.

Model of the permanent magnet synchronous generator

The mathematical model for the PMSG on the rotating reference d - q frame can be found in the literature [1], [6], [16] as:

$$(1) \quad \frac{d}{dt} i_d = \frac{1}{L_d} V_d - \frac{R_s}{L_d} i_d + \frac{L_q}{L_d} p \omega i_q,$$

$$(2) \quad \frac{d}{dt} i_q = \frac{1}{L_q} V_q - \frac{R_s}{L_q} i_q - \frac{L_d}{L_q} p \omega i_d - \frac{\Phi_m p \omega}{L_q},$$

$$(3) \quad T_e = \frac{3}{2} p \left[\lambda i_q + (L_d - L_q) i_d i_q \right],$$

where L_d and L_q are the d and q axis inductances, R_s is the resistance of the stator windings, i_d and i_q are the d and q axis currents, V_d and V_q are the d and q axis voltages, ω is the angular velocity of the rotor in radians per second, Φ_m is the amplitude of the flux induced by the permanent magnets of the rotor in the stator phases, p in the number of pole pairs, and T_e is the electromagnetic torque.

L_d and L_q inductances represent the relation between the phase inductance and the rotor position due to saliency of the rotor. For example, the inductance measured between phase a and b (phase c is left open) is given by:

$$(4) \quad L_{ab} = L_d + L_q + (L_q - L_d) \cos \left(2\theta_e + \frac{\pi}{3} \right),$$

where θ_e is the electrical angle.

For a round rotor the phase inductance is:

$$(5) \quad L_d = L_q = \frac{L_{ab}}{2},$$

where L_{ab} is the inductance measured between phase a and b (phase c is left open).

The mechanical part of the model is given by:

$$(6) \quad \frac{d}{dt} \omega_m = \frac{1}{J} (T_e - T_m).$$

This kind of the PMSG model, is used in Simulink's SimPower System toolbox and other well-known simulation software (PSIM, PLECS, etc.).

Another model named trapezoidal, also widely used in the simulation software, was described in detail in [16].

Model of the small wind turbine

One of the most important aspects during analysis of the wind energy conversion system (WECS) is the proper model of the wind turbine (WT).

The model of the WT is based on the following equation from [17] and [18]:

$$(7) \quad C_p(\lambda, \beta) = c1 \cdot \left(\frac{c2}{\lambda_i} - c3 \cdot \beta - c4 \right) \cdot e^{-\frac{c5}{\lambda_i}} + c6 \cdot \lambda,$$

where: $c1=0.5176$, $c2=116$, $c3=0.4$, $c4=5$, $c5=21$, $c6=0.0068$. These are approximation coefficients obtained empirically (regression from wind tunnel measurements) or from the blade element method [19].

Since this will be the model of a SWT, the blade's pitch angle is fixed (no pitch angle control) therefore $\beta = 0$. From [20] the calculation of λ_i is:

$$(8) \quad \frac{1}{\lambda_i} = \frac{1}{\lambda + 0.08 \cdot \beta} - \frac{0.035}{\beta^3 + 1}.$$

From (7) is visible that C_p only depends on the tip speed ratio (λ) since the pitch angle β equals zero as mentioned before. The relationship between the rotational speed and the wind speed is described as:

$$(9) \quad \lambda = \frac{\omega R}{v},$$

where ω is the rotational speed in radians per second, R is the rotor radius in meters and v is the wind speed in meters per second. The value of tip speed ratio λ is unitless.

The inputs for the turbine model are rotational speed ω of the shaft and the wind speed v . As an output of the WT model is the mechanical torque T_m generated by the turbine which is related to C_p as:

$$(10) \quad T_m = \frac{P_{wind} C_p}{\omega} = \frac{0.5 \rho \pi R^2 v^3 C_p}{\omega},$$

where P_{wind} is the theoretical power obtainable from the wind and is based on the transversal area of the rotor times the power coefficient C_p which depends on aerodynamic approximation coefficients $c1$ to $c6$.

Also, in (10) notice that P_{wind} is the area of the turbine times the air density ρ divided by 2 and multiplied by the cube of the wind speed (from the kinetic energy of the wind). This power divided by the rotational speed gives the torque generated by the turbine. For this model of the wind turbine the maximum C_p is 0.48 for an optimal tip speed ratio λ_{opt} of 8.1, notice that these quantities are unitless. This C_{p_max} is in accordance with the Betz's limit (<0.59) and the aerodynamic characteristics of three bladed turbines according to [21].

The turbine power characteristics for this wind turbine with a $C_{p_max}=0.48$ and a $\lambda_{opt}=8.1$ are presented in Figure 1.

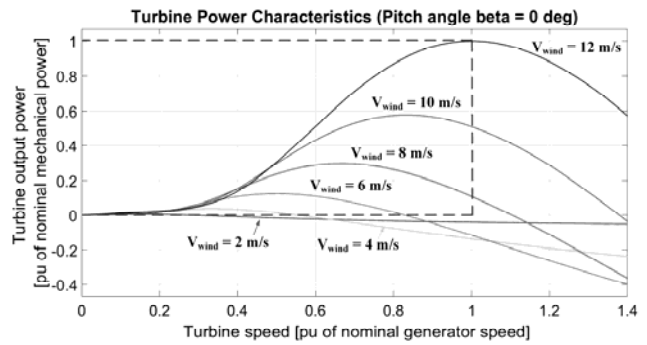


Fig. 1. Aerodynamic characteristic of the wind turbine

Maximum Power Point Tracking algorithm for a SWT

The addition of a switching device (power electronics) is to obtain the maximum power point tracking (MPPT) with the given generator and the wind turbine model described before. The MPPT is done with a passive rectifier and boost converter, as Fig. 2 shows. This allows the generator to operate in the low speed region (lower than the nominal speed), this means that the wind turbine will also generate power at low wind speeds.

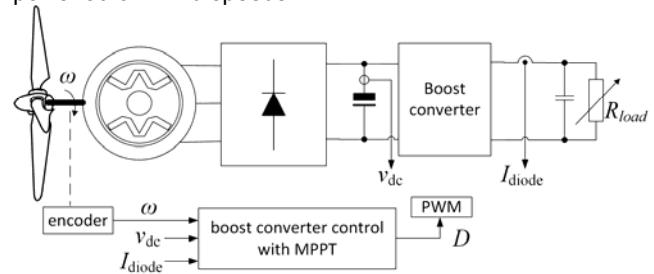


Fig. 2. Circuit schematic of the WECS for MPPT

The optimal torque control (OTC) method was chosen due to its fast dynamic response and high efficiency as shown in [22]. This tracking algorithm calculates the optimal torque as:

$$(11) \quad T_{opt} = \frac{0.5 \pi \rho C_{p_max} R^5}{\lambda_{opt}^3} \cdot \omega^2,$$

where $C_{p_max} = 0.48$ and $\lambda_{opt} = 8.1$, as stated before, air density ρ is 1.13 kg/m^3 , rotor radius R is 0.8 m , and ω is the feedback signal of the rotational speed.

From (11) the current reference for the boost converter controller is calculated as:

$$(12) \quad I_{ref} = \frac{P_{max}}{v_{in}} = \frac{T_{opt} \cdot \omega}{v_{in}},$$

where P_{max} is the theoretical maximum power obtained from the turbine, v_{in} is the DC bus voltage at the output of the passive rectifier (input of the converter), and T_{opt} is calculated from (15). The I_{ref} and the current feedback I_{diode} are the inputs to the PI controller of the boost converter.

Methodology of co-simulation

The general idea of this method is presented on Fig. 3.

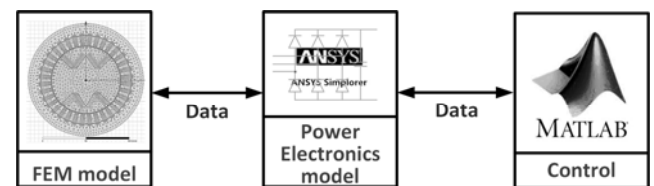


Fig. 3. Idea of the Co-Simulation with more than two software programs

As shown in section 2, classical simulation analysis of the electrical machines uses many simplifications. Normally, electrical machine models are first order differential equations (1) to (3) and (7) to (10). With these, it is not possible to analyze nonlinear behavior like saturation or demagnetization, etc.

In the co-simulation the subsystems (FEA model, Power Electronics circuit, and the control loop) will exchange data as shown in Fig. 3. Co-Simulation has an advantage in calculation of multi-domain systems. This method is also flexible and allows consideration of multiple technical problems with different calculation steps, at the same time, although the main time step is defined by the circuit model (Power electronics model) as can also be inferred from Fig. 3. Because the model is calculated by more than one system, it is possible to model complex and large-scale objects.

The details of the generator and the boost converter are given in Table 1.

Table 1. Parameters and values of the co-simulation

Turbine Aerodynamics	
Rotor radius	0.8 m
Maximum power coefficient $C_{p\max}$	0.48
Optimal tip speed ration λ_{opt}	8.1
C_p - λ curve approximation coefficients	$c1=0.5176, c2=116, c3=0.4, c4=5, c5=21, c6=0.0068$
PMSG	
Pole pairs	2
Nominal power	3000 W
Nominal speed	1500 rpm
Stator phase resistance	5.56 ohm
Stator phase inductance	4.11 mH
Inertia	$0.015 \text{ kg}\cdot\text{m}^2$
Viscous damping	$0.0004924 \text{ N}\cdot\text{m}\cdot\text{s}$
Boost converter	
PWM frequency	100 Hz
Inductor	320 mH
Input capacitor	1000 μF
Output capacitor	1370 μF
Load	240 ohms

The same parameters were used for both simulation and co-simulation. Notice that the pulse width modulation (PWM) frequency is left at 100 Hz, this is due to the co-simulation computation time, the higher the frequency the longer the co-simulation will take to compute since more time steps will be needed. For this co-simulation a 0.1 ms time step was used, this is similar to the time step used in [12]. Co-Simulation model was shown in Fig. 4.

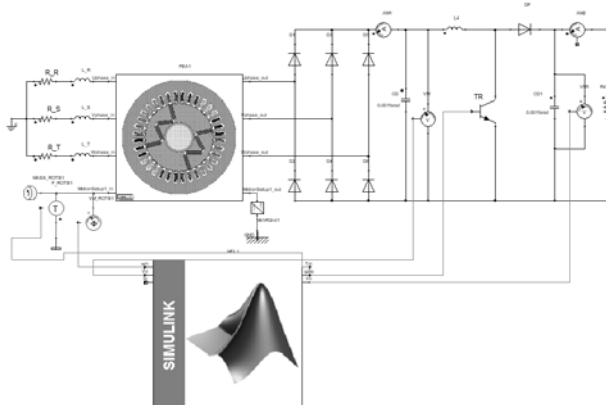


Fig. 4. Schematic diagram of the co-simulation of the PMSG SWT with boost converter

As shown in Fig. 4, the control and modelling of the wind turbine are done within the Matlab Simulink environment, this is useful to compare with the results of the SimPower systems toolbox's simulation. As an output from the Matlab Simulink block is the mechanical torque exerted to the generator from the wind turbine's blades. This is a direct driven wind turbine; therefore, no gearbox ratio is needed. Additionally, the switching signal for the transistor is shown as an output.

Also, in Fig. 4 the inputs of the control block are the boost converter's input voltage, output voltage and the generator's shaft mechanical speed ω .

In Fig. 5 the schematic diagram of the wind turbine with passive rectifier and boost converter is shown (made in the SimPower systems' toolbox). Notice the SimPower systems' toolbox models for the electrical circuit. It is important to mention that all parameters were the same for the simulation and the co-simulation.

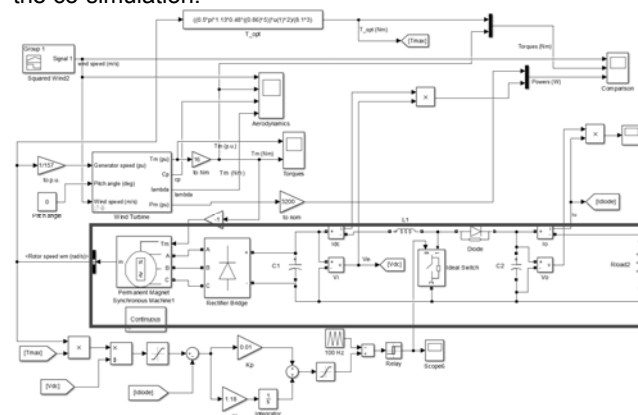


Fig. 5. Schematic diagram of the boost converter's control and the wind turbine model for the co-simulation

Analysis of SWT operation using simulation and co-simulation approach

In Fig. 6 the input (wind speed) of the simulation and co-simulation is shown, this staircase signal type is useful to assess the control properties.

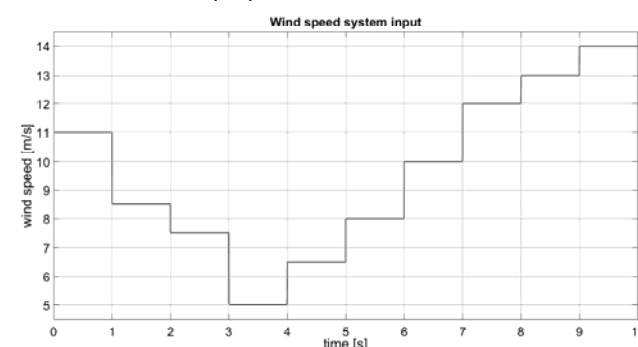


Fig. 6. Wind speed as system input for simulation and co-simulation

In Fig. 7 the results of the simulation are shown. Input signal of the system (wind speed) is the same for both simulation and co-simulation. For simulation purposes the input signal is varied in discrete steps although the wind does not vary in this manner, the boost converter is able to maintain the C_p close to 0.48 as the blade's maximum power characteristic. In Fig. 7a notice that at 12 m/s the nominal power is achieved. In Figure 7d, although the steady wind steps are not long enough to achieve steady state, still, the controller tries to maintain the WT spinning at 8.1 tip speed ratio (λ).

In Fig. 8 the results of the co-simulation are shown. In comparison with the simulation results (Fig. 7) the power at the output does not achieve the nominal power of 3 kW.

This is related to the results in Fig. 9. The PMSG reaches a 10 A amplitude in the phase currents and the saturation does not allow for the boost converter to keep the MPPT operation of the turbine, therefore Fig. 8c and Fig. 8d show a stalled behaviour of the WT.

Notice that in Fig. 8a there is a ripple in the power output, even when the system is under control (before 7 seconds). This is related to the PMSG torque ripple, and since the generator is directly connected to the WT blades, this is also visible in Fig. 8d.

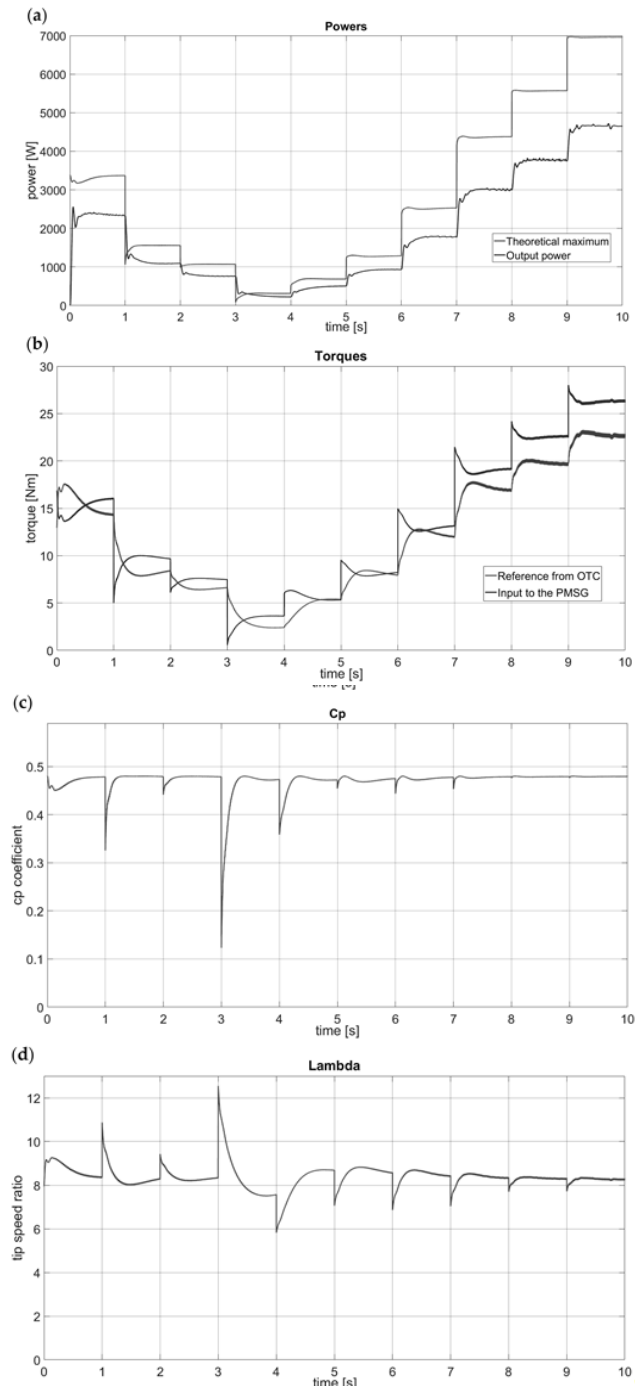


Fig. 7. Results from the Simulink SimPower system's simulation (a) power, (b) torque, (c) power coefficient C_p , (d) tip speed ratio λ

It is possible to obtain the maximum power of WT in co-simulation using slightly larger blades (0.86 m).

As explained before, the reason for such a behaviour of the WT in the co-simulation is connected to the PMSG model. In the co-simulation, the complete geometry and

material properties are stated, which means that the core saturation is present. Once the control algorithm asks for higher currents, higher than 10 A according to Fig. 9b, then the PMSG just stalls the WT.

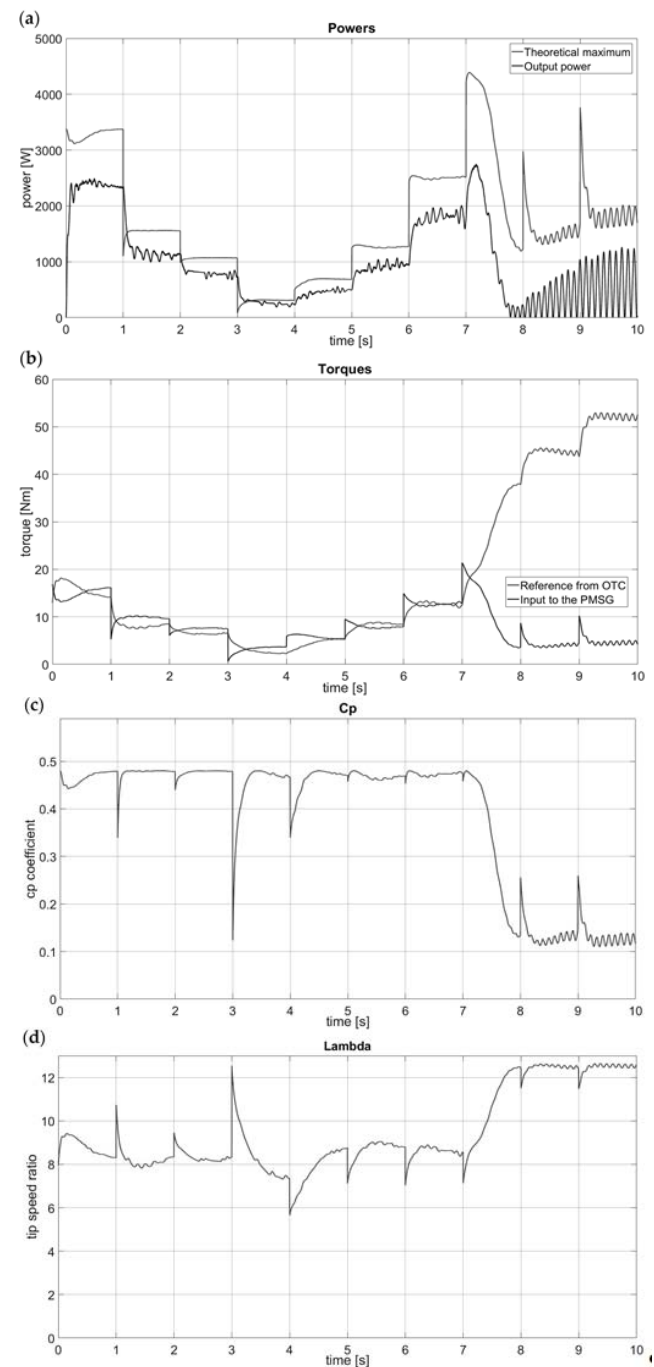


Fig. 8. Results from the FEA Co-simulation (a) power, (b) torque, (c) power coefficient C_p , (d) tip speed ratio λ

Notice in Fig. 10a and Fig. 10b that, even though the rotational speed ω is higher in the co-simulation, the PMSG is not able to maintain the DC bus voltage (Fig. 11) and the output power falls, leaving the turbine in a stall state. This is evident from Fig. 8c and Fig. 8d.

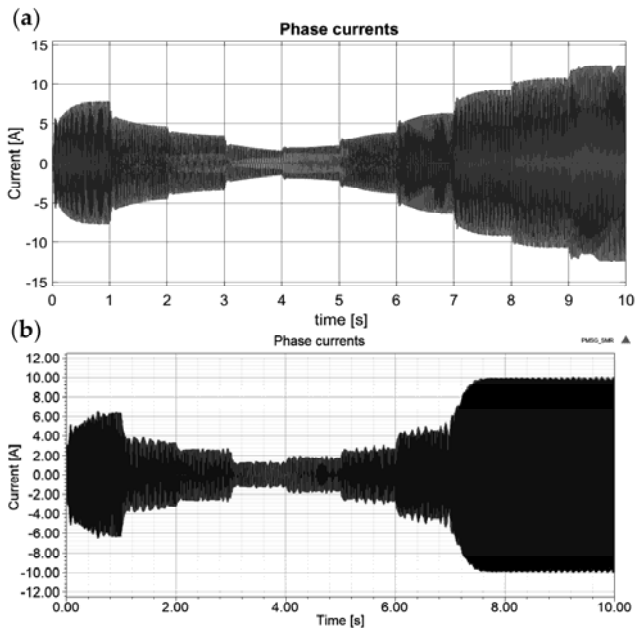


Fig. 9. Phase currents from (a) simulation and (b) co-simulation

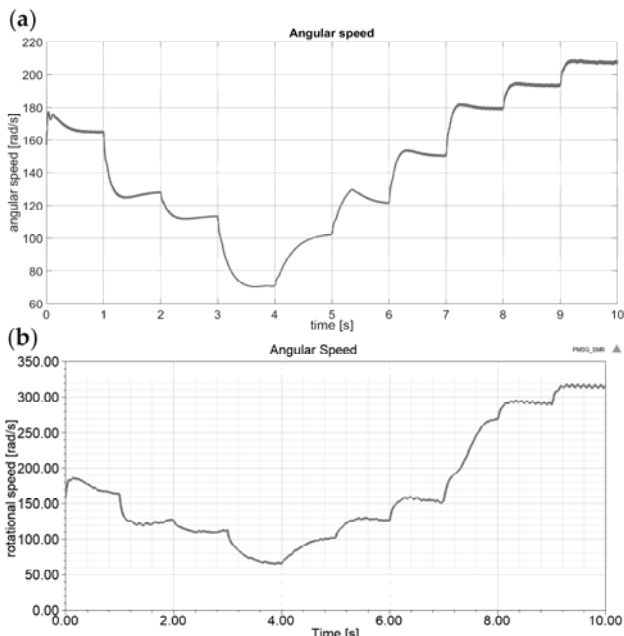


Fig. 10. Angular speed in radians per second from (a) simulation and (b) co-simulation

Discussion

Even though, special attention was put on the tuning of the parameters of the SimPower system's model is evident that the simulation results are not able to estimate correctly the behaviour of the coupling between the aerodynamic wind turbine model and the PMSG.

From the initial results some modifications to improve the system's behavior at high wind speeds were done. These corroborated that the turbine was able to produce the 3 kW previously predicted in the PMSG design phase. It is important to mention that since the PMSG is based on the Sh-90L4 induction motor (same stator and windings), is not advisable to run the phases at 10 A, as shown in the simulation and co-simulation, for a long time. The original IM Sh-90L4 is able to withstand 18 A of starting current according [23].

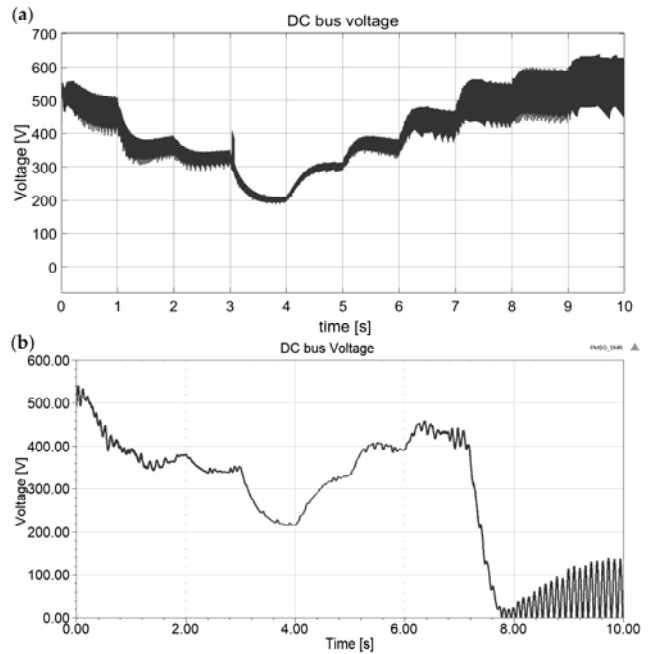


Fig.11. DC bus voltage before boost converter from (a) simulation and (b) co-simulation

Conclusions

From the results shown in the analysis of SWT operation section it can be concluded that the co-simulation brings to the analysis of the design of complex interconnected systems a very powerful tool with a high level of resolution in the output signals. This makes the co-simulation approach a very important area of development in future research.

On the other hand, the co-simulation is still more time consuming than the typical simulation. For example, for co-simulating 10 seconds on a core i7 desktop computer with 8 Gb of memory the complete computational time was 12 hours. This is because as was described in [4], [10], [12], and [24] at each time step the software converts the values of the nodes on the circuit to loops (Norton equivalent to Thevenin equivalent) and vice versa. Therefore, this transformation and the computational time the FEA takes to post the outputs is constant at each time step and could take several seconds per time step.

R. E. Quintal-Palomo thanks the funding from the Mexican Council of Science and Technology CONACYT and the Department of research, innovation and higher education of the Yucatan State SIIES through grant number 312140. The computations were performed using the resources of the Wrocław Centre for Networking and Supercomputing (<http://wcss.pl>). Grant No. 400

Authors: MSc. Roberto Eduardo Quintal Palomo Universidad Autónoma de Yucatán, Facultad de Ingeniería, Mérida, Yucatán, México E-mail: roberto.quintal@correo.uady.mx; prof. dr hab. inż. Mateusz Dybkowski Politechnika Wroclawska, katedra maszyn, napędów i pomiarów elektrycznych ul. Smoluchowskiego 19, 50-372, Wrocław, E-mail: mateusz.dybkowski@pwr.edu.pl;

REFERENCES

- [1] J. Gieras, *Permanent Magnet Motor Technology*, 3rd ed., vol. 20096073. CRC Press, 2009.
- [2] D. Casadei *et al.*, "Detection of magnet demagnetization in five-phase surface-mounted permanent magnet generators," in *2012 3rd IEEE International Symposium on Power Electronics for Distributed Generation Systems (PEDG)*, 2012, pp. 841–848.

- [3] M. P. Kazmierkowski, R. Krishnan, and F. Blaabjerg, *Control in Power Electronics*. Elsevier, 2002.
- [4] P. Zhou, D. Lin, W. N. Fu, B. Ionescu, and Z. J. Cendes, "A general cosimulation approach for coupled field-circuit problems," *IEEE Trans. Magn.*, vol. 42, no. 4, pp. 1051–1054, Apr. 2006.
- [5] N. a. Orlando, M. Liserre, and A. Dell'Aquila, "Management of power excess in wind turbine system," *2009 13th Eur. Conf. Power Electron. Appl.*, 2009.
- [6] B. Wilamowski and D. Irwin, *The industrial electronics handbook*, 2nd ed. CRC press, 2011.
- [7] Wenxiang Zhao, Ming Cheng, Xiaoyong Zhu, Wei Hua, and Xiangxin Kong, "Analysis of Fault-Tolerant Performance of a Doubly Salient Permanent-Magnet Motor Drive Using Transient Cosimulation Method," *IEEE Trans. Ind. Electron.*, vol. 55, no. 4, pp. 1739–1748, Apr. 2008.
- [8] J. Zhao, X. Gao, B. Li, X. Liu, and X. Guan, "Open-Phase Fault Tolerance Techniques of Five-Phase Dual-Rotor Permanent Magnet Synchronous Motor," *Energies*, vol. 8, no. 11, pp. 12810–12838, Nov. 2015.
- [9] Y. Cetinceviz, D. Uygun, and H. Demirel, "Multi-criterion design and 2D cosimulation model of 4 kW PM synchronous generator for standalone run-of-the-river stations," in *2015 International Conference on Renewable Energy Research and Applications (ICRERA)*, 2015, vol. 5, pp. 1470–1476.
- [10] M. Fitouri, Y. Bensalem, and M. N. Abdelkrim, "Analysis and co-simulation of permanent magnet synchronous motor with short-circuit fault by finite element method," *13th Int. Multi-Conference Syst. Signals Devices, SSD 2016*, pp. 472–477, 2016.
- [11] M. Fitouri, Y. Bensalem, and M. N. Abdelkrim, "Modeling and detection of the short-circuit fault in PMSM using Finite Element Analysis," *IFAC-PapersOnLine*, vol. 49, no. 12, pp. 1418–1423, 2016.
- [12] Z. Peng, L. Chai, and Y. Sheng, "Co-simulation modeling and fault diagnosis of closed-loop squirrel-cage motor systems," in *2017 12th IEEE Conference on Industrial Electronics and Applications (ICIEA)*, 2017, pp. 718–722.
- [13] K.-C. Kim, "Analysis on Core Loss of Brushless DC Motor Considering Pulse Width Modulation of Inverter," *J Electr Eng Technol*, vol. 9, no. 6, pp. 1914–1920, 2014.
- [14] P. Makolo, "Wind Generator Co-Simulation with Fault Case Analysis Master of Science Thesis," Chalmers University of Technology, Göteborg, 2013.
- [15] C. Wang, X. Liu, and Z. Chen, "Incipient stator insulation fault detection of permanent magnet synchronous wind generators based on hilbert-huang transformation," *IEEE Trans. Magn.*, vol. 50, no. 11, 2014.
- [16] MathWorks, "SimPower Systems PMSG Model," *Permanent Magnet Synchronous Machine*, 2018. [Online]. Available: <https://www.mathworks.com/help/phymod/sps/powersys/ref/permanentmagnetsynchronousmachine.html>. [Accessed: 30-Nov-2018].
- [17] D. Rekioua, *Wind Power Electric Systems*, 1st ed. London: Springer London, 2014.
- [18] S. Heier, *Grid Integration of Wind Energy*, 3rd ed. Chichester, UK: John Wiley & Sons, Ltd, 2014.
- [19] D. Wood, *Small Wind Turbines*, 1st ed. London: Springer London, 2011.
- [20] P. D. Clausen and D. H. Wood, "Recent Advances in Small Wind Turbine Technology," *Wind Eng.*, vol. 24, no. 3, pp. 189–201, May 2000.
- [21] E. Hau, *Windkraftanlagen*: Springer, 2000.
- [22] M. Heydari and K. Smedley, "Comparison of maximum power point tracking methods for medium to high power wind energy systems," in *2015 20th Conference on Electrical Power Distribution Networks Conference (EPDC)*, 2015, no. April, pp. 184–189.
- [23] C. Indukta, "Sh 90L4," *Sh90-L4 Electrical parameters*, 2019. [Online]. Available: <https://www.cantonigroup.com/celma/en/page/offer/details/1/146/Sh90L-4>. [Accessed: 11-Mar-2019].
- [24] C. M. Apostoia and M. Cernat, "Fault detection in synchronous motor drives, a co-simulation approach," *Jt. Int. Conf. - ACEMP 2015 Aegean Conf. Electr. Mach. Power Electron. OPTIM 2015 Optim. Electr. Electron. Equip. ELECTROMOTION 2015 Int. Symp. Adv. Electromechanical Moti*, pp. 617–622, 2016.